MODELING ION ACCELERATION IN A Z-PINCH BY AN M=0 INSTABILITY WITH HALL-MHD

Julio J. MARTINELL and Rosa M. FAJARDO

Instituto de Ciencias Nucleares,
National Autonomous University of Mexico
A. Postal 70-543, México D.F., MEXICO

Ions acceleration by an m=0 instability in a z-pinch is modeled using the Hall-MHD theory taking into account that the axial plasma velocity developed during the instability. We make a numerical solution of the equations which shows that the instability develops until the narrowing neck is stopped by the increased pressure. For typical plasma focus parameters, the final neck radius is about one fourth of the initial radius. Since the model has an intrinsic axial asymmetry, the resulting electric field points everywhere towards the cathode, irrespective of the neck position. This E-field, combined with the B-field, is used to compute ion trajectories, using the equation of motion for a single particle. We considered the motion of two classes of particles: singular particles that cross the cylinder axis and off-axis regular particles. They move in opposite directions on average and the energy gain of singular orbit ions is larger, reaching values of up to sixty.

Keywords: MHD instabilities, ion acceleration, z-pinch, Hall-MHD theory, dense plasma focus

1. Introduction

Nuclear fusion reactions in a z-pinch or in a plasma focus are mainly due to a beam-target process resulting from ions accelerated during the discharge, as opposed to thermonuclear interactions. Quite different models for ion acceleration have been proposed over the years based on various effects, ranging from the induction of an E-field due to the symmetric compression of the B-field (e.g. [2, 3]), to the different fields produced by plasma instabilities ([4, 5]). It is likely that more than one acceleration mechanism is in effect during the discharge. In a model based on the development of the m=0 instability proposed by Haines [1], the existence of an asymmetry along the z-axis was pointed out, which causes ions near the symmetry axis to be preferentially accelerated. This arises from the average axial drift of off-axis ions due to the radial electric field $Zn_ieE_r = \partial p_i/\partial r$. This axial flow has to be balanced by an equal and opposite flow of ions on-axis that have singular orbits.

To account for this effect it is necessary to include the Hall term in Ohm's law, as well as the electron pressure term, since these are the ones that break the symmetry. However, the assumption of no longitudinal plasma flow made in ref.1 is inconsistent with momentum equations, as we will show. We consider here a model based on Haines' idea, that allows a finite axial velocity to develop as the instability grows. Our model solves the Hall-MHD equations for a cylindrical plasma column, initially in equilibrium, after a pinching perturbation is applied.

author's e-mail: martinel@nucleares.unam.mx

2. Model for the m=0 instability

In order to determine the ion orbits and obtain the acceleration they experience, we first need to model the evolution of the m=0 instability of the plasma column. To do this, we use a Hall-MHD model, as this is the one that accounts for the asymmetry along the axial direction resulting from the singular orbit ions; the Hall and the electron pressure gradient terms in Ohm's law have mixed parities. There have been few works that have considered Hall-MHD to analize the dynamics and stability of a z-pinch (see e. g. ref.6 and references therein). The one we consider here is a reduced model that neglects thermal conductivity and, unlike ref.6, we do not study the stability conditions, but start from a potentially unstable equilibrium state. Our aim is mainly to estimate the electric fields produced by the instability including the Hall term, during the development of the instability and we do not expect them to be much influenced by the inclusion of heat transfer, due to the fast collapse time. For the analysis, we use a cylindrical plasma column having complete axisymmetry (i.e. $\partial/\partial\theta = 0$), carrying a uniform axial current I, with radius a and an azimuthal magnetic field $\mathbf{B} = B_\theta(r)\hat{\theta}$, given by $B_\theta = 2Ir/ca^2$ for $r < a$ and $B_\theta = 2I/cr$ for $r > a$. The corresponding equations for the density ρ, radial velocity v_r and axial velocity v_z, are,

$$\frac{\partial\rho}{\partial t} = -\frac{1}{r}\frac{\partial}{\partial r}(r\rho v_r) \quad - \quad \frac{\partial}{\partial z}(\rho v_z) \quad (1)$$

$$\rho\left(\frac{\partial v_r}{\partial t} + v_r\frac{\partial v_r}{\partial r} + v_z\frac{\partial v_r}{\partial z}\right) = -\frac{\partial p}{\partial r}$$

$$-\frac{J_z B_\theta}{c} \quad (2)$$

$$\rho \left(\frac{\partial v_z}{\partial t} + v_r \frac{\partial v_z}{\partial r} + v_z \frac{\partial v_z}{\partial z} \right) = -\frac{\partial p}{\partial z}$$
$$+ \frac{J_r B_\theta}{c} \quad (3)$$

where $J_r = (Ir/\pi a^3)\partial a/\partial z$, and $J_z = (I/\pi a^2)$. As the plasma evolves, the associated electric fields are obtained from Ohm's law as,

$$E_r = \frac{v_z B_\theta}{c} + \eta J_r - \frac{J_z B_\theta}{nec} - \frac{1}{ne}\frac{\partial p_e}{\partial r} \quad (4)$$

$$E_z = -\frac{v_r B_\theta}{c} + \eta J_z + \frac{J_r B_\theta}{nec} - \frac{1}{ne}\frac{\partial p_e}{\partial z} \quad (5)$$

where η is the resistivity. The system is closed using a polytropic equation for the pressure: $p = k\rho^\gamma$ with γ a free parameter. In this model the B-field is frozen to the electrons and thus there is a difference between the guiding-center and the center-of-mass velocities. As a result, the perturbation neck can slowly drift along the $-z$-direction.

The evolution of the column radius $a(t)$ follows from Faraday's law. In addition, we keep a finite v_z as opposed to Haines' consideration who used $v_z = 0$ [1], which is inconsistent with the formation of a neck in the column. The existence of an axial flow is essential. Therefore, the equation for a is,

$$\frac{\partial a}{\partial t} = \frac{a^3}{2}\frac{\partial}{\partial z}\left(\frac{v_z}{a^2}\right) + \frac{\eta c^2}{4\pi}\frac{\partial^2 a}{\partial z^2} - \frac{3\eta c^2}{4\pi a}\left(\frac{\partial a}{\partial z}\right)^2$$
$$-\frac{mIa^3}{2\pi e}\frac{\partial}{\partial z}\frac{1}{\rho a^4} + \frac{a}{2r}\frac{\partial}{\partial r}(rv_r)$$
$$-\frac{mI}{2\pi e r a^2}\frac{\partial a}{\partial z}\frac{\partial}{\partial r}\left(\frac{r^2}{\rho}\right) \quad (6)$$

Here we also assumed that the electron pressure follows a polytropic equation of the type used for the total pressure ($p_e = k_e \rho^{\gamma_e}$), which causes it not to appear in Eq.(6). The reason why the assumption of $v_z = 0$ is inappropriate can be understood if we take $v_z = 0$ in Eq.(3) giving,

$$\frac{\partial p}{\partial z} = \frac{J_r B_\theta}{c}$$

Then we substitute the expressions of J_r and B_θ in terms of $a(z)$ and the polytropic equation for p and obtain the proportionality,

$$\frac{da}{dz} \propto \frac{\partial \rho}{\partial z}.$$

However, the neck formation should produce the opposite effect since as one moves along z to the narrow region ($da/dz < 0$) the density should increase ($\partial\rho/\partial z > 0$). Thus a finite value of v_z is necessary.

Equations (1, 2, 3, 6) are solved in a domain that includes the plasma and the vacuum region, covering the range $r = (0, L)$ and $z = (-L, L)$. This region represents a single neck (the pressumed "hot spots") which we assume is part of a periodic sequence. The

electric fields are computed only within the plasma region, since in the vacuum surrounding the neck they are zero. The plasma particles cannot reach the vacuum region because of the strong electrostatic forces. Only when the ions are accelerated to very high energies can they leave the plasma.

The numerical scheme followed is based on a leapfrog trapezoidal algorithm, with a predictor-corrector evolution. The boundary conditions in the z direction are periodic for all variables except v_z, for which we set its derivative to be zero. This is imposed to avoid axial plasma acceleration at the domain boundary and assure a periodic behavior for v_z. In the radial direction we imposed Newmann boundary conditions at $r = 0$ (zero derivative), while for the vacuum region we assumed free-flow boundary conditions. The perturbation is applied as a small sinusoidal radial velocity: $v_r(r, z, t = 0) = V_{r0}r \cos(kz)$. The free parameters that we can vary are the total current I and the pressure P. In the calculations presented here we used $V_{r0} = 0.75$ (normalized to L/t_0). For the initial density profile we tested both flat and parabolic dependencies; for the latter profile we considered two different situations: that when the column is initally in equilibrium and when it is out of equilibrium. In the following we show results for parabolic profiles, as flat profiles do not produce qualitative differences.

In Fig.1 we show the results for the plasma column density for $I = 180kA$ and $P = 3.7 \times 10^7 dyn/cm^2$. This produces the maximum compression rate at the neck at a time of 20 ns. The values of the polytropic index were varied and the best compression was obtained for $\gamma = 2$ corresponding to a 2D adiabatic evolution, as expected. Here, the plasma was assumed in MHD equilibrium at the time of the perturbation; in this case the density sharply increases at the plasma boundary during compression and stays relatively constant down to the center. This is in contrast to the case in which there is no initial equilibrium, with a pressure 100 times higher, shown in Fig.2. The compression is slower, reaching maximum values at 38 ns, and the density is strongly peaked at the center. The same evolution of the m=0 instability is shown for the velocity field, in Fig.3 for the equilibrium case. It noticed that an axial velocity is present near $r = 0$, in addition to the inward component near the plasma boundary; as expected it has odd parity in z. Finally, in Fig.4 we show the electric field vectors for the equilibrium profile, where one can see that they are maximum near the edge at the neck, but it has also an important magnitude at the center, parallel to the z-axis. This is more evident for the high density case shown in Fig.5. There is a manifest asymmetry along z, since the E-field magnitude is larger on the right side of the neck than on the left, and this is due to the influence of the Hall term.
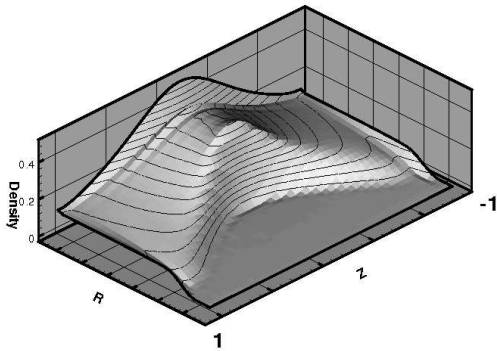
DENSITY DISTRIBUTION

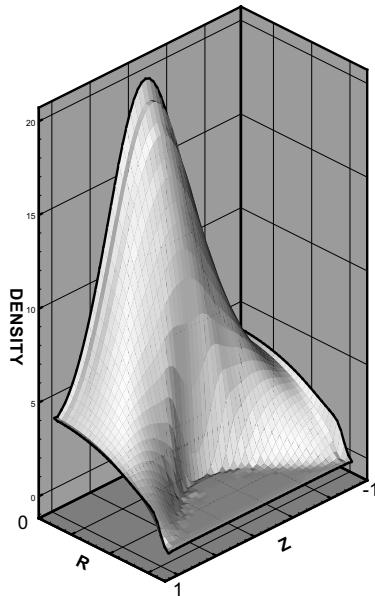Fig. 1 Plasma density $\rho(r, z)$ in the column near the late stages of the instability.

Fig. 2 Density profile for a high initial pressure, out of equilibrium, near the end of the compression.

3. Ion orbits

Once the m=0 instability develops, the resulting electromagnetic fields act upon the charged particles, and thus ions can eventually be accelerated. In order to obtain the ion orbits and determine the acceleration rate we solve the ion motion equations for a single particle, which in cylindrical coordinates are.

$$\frac{\partial v_r}{\partial t} = \frac{Ze}{m_i}(E_r - v_z B_\theta) + \frac{h}{r^3} \qquad (7)$$

$$\frac{\partial v_z}{\partial t} = \frac{Ze}{m_i}(E_z - v_r B_\theta) \qquad (8)$$

where $h = r^2\dot{\theta}$ is the specific angular momentum, a constant of motion. As mentioned above, near the region of neck formation there are two kinds of particle orbits drifting in opposite directions: off-the-axis
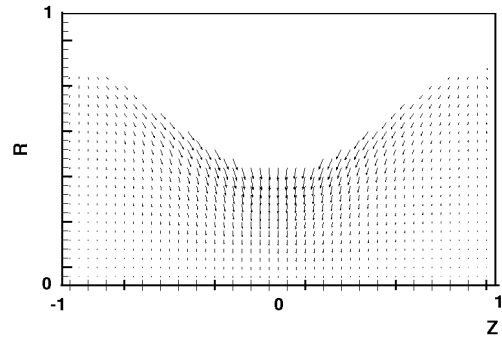
PLASMA VELOCITY VECTORS

Fig. 3 Velocity vectors at the end of the instability.
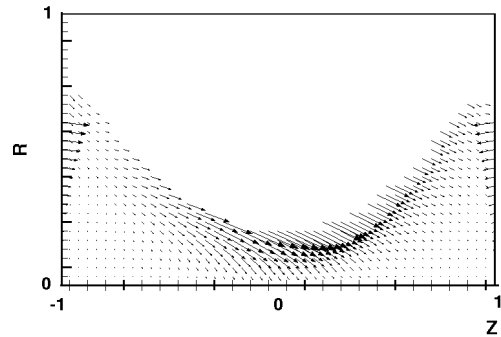
ELECTRIC FIELD VECTORS

Fig. 4 Electric field vectors from Ohm's law with Hall term for initial pressure equilibrium.

ions drifting from cathode to anode and singular-orbit ions located within a Larmor radius of the axis. The latter are less numerous but have higher speeds. We have solved numerically Eqs.(7), (8) for the electric and magnetic fields obtained from the instability development, confirming the presence of the two types
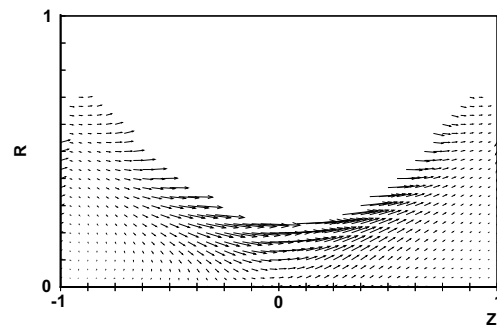
ELECTRIC FIELD VECTORS

Fig. 5 Electric field vectors at the end of the instability for high pressure case.

of orbits. The E-fields used were those for the high density evolution.

In Fig.6 we show the orbit of an off-axis ion starting at $(r_0, z_0) = (0.4, -0.6)cm$ with an energy $W = 80eV$ and velocity vector having a pitch angle of 45° with the cylinder axis, shown with continuous line. There is a grad-B drift to the left but there is practically no energy gain as it can be evidenced by the velocity path shown in the same figure by the dashed line. The distance from the origin is a measure of the ion speed, and hence, the energy. Now, for ions located close to the axis (less than one gyroradius, which in the vicinity of the axis, where B=3T, is of the order of 0.03 cm) the orbit is snake-like moving to the right, regardless of which side of the neck it starts from, as it can be seen in Fig.7. The ion energy is $80eV$ and has a pitch angle of 45°. It starts at the left side of the neck and it is followed until it leaves the instability region. The energy gained by the ion is appreciated in the velocity trajectory plot depicted by the dotted line in the same figure: the distance from the origin keeps increasing. In a couple of orbits the ion energy goes up by a factor of 23 to $1.8keV$. It is also apparent that the velocity increases predominantly to the z-direction and thus the pitch angle gets reduced on each cycle. This is characteristic of an axial acceleration produced by the axial electric field.

There is a third type of ion orbit which we found to be the most common of all. It is possible for an ion to transit from an off-axis orbit to a singular orbit when the starting point is close to the a region where the E-filed has a large axial component. This mixed orbit is shown in Fig.8 which starts being non-singular, but drifts towards the column axis as a result of the $E \times B$ drift; it then crosses the axis and the orbit becomes singular and starts gaining energy. Here the trajectory starts exactly at the neck ($z = 0$) with the same pitch angle as the previous cases (45°) and the initial energy is $W = 0.2keV$. The velocity space evolution (dashed curve) shows again the change in orbit type and how energy is increased, just as the symmetry axis is reached. This time there is a 7.5-fold energy gain, reaching an energy of $1.5keV$ at the time the ion leaves the simulation region.

However, for ions starting on the left of the neck, close to the plasma edge, the energy increase can be quite large since they cross most part of the plasma column. Fig.9 is an example of an orbit with an energy gain of 61, which first meanders towards the axis and ends up with a final energy of $6.1keV$, as it leaves the simulation region (shown by dotted box).

4. Conclusions

The model for the m=0 instability developed here based on Hall-MHD, produces electric fields that give
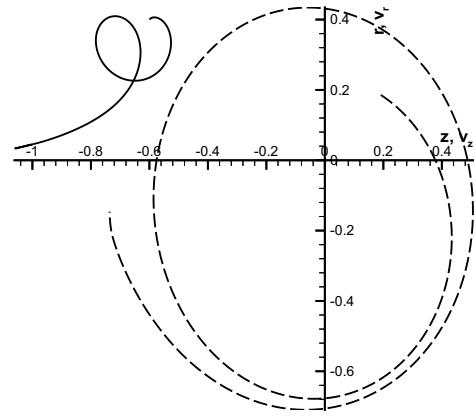

Fig. 6 Off-axis ion orbit (solid line) with energy 80 eV, drifting to the left and velocity space trajectory (dashed line).
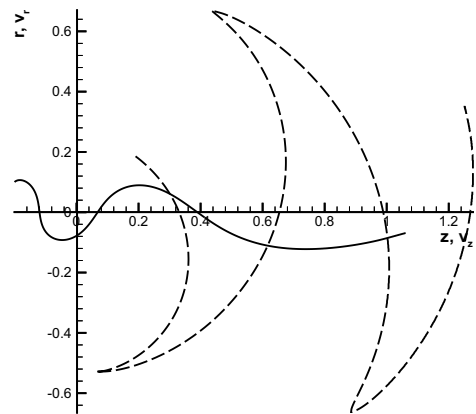

Fig. 7 Singular orbit (solid) of ion on-axis with energy 0.1 keV drifting to the right and velocity path (dashed).

an asymmetry in the z-direction, being always directed towards the cathode on both sides of the plasma neck but larger in magnitude on the positive z-axis. They are mainly concentrated near the plasma edge close to the column neck, but are important on the symmetry axis too. This field mainly accelerates ions with on-axis orbits but a great part of off-axis ions drift to these orbits, especially those to the right of the neck. Some ions on the left side do not get accelerated. The inclusion of the axial plasma velocity in the model is found to be quite important as this is responsible of a contribution to the E_r field component that opposes that of the Hall term. E_r can thus be inverted. This causes off-axis ions not to accelerate much. Only ions close to the axis can travel along the plasma column and are accelerated along the cathode direction. They are presumably responsible for the beam-target fusion reactions. The energy
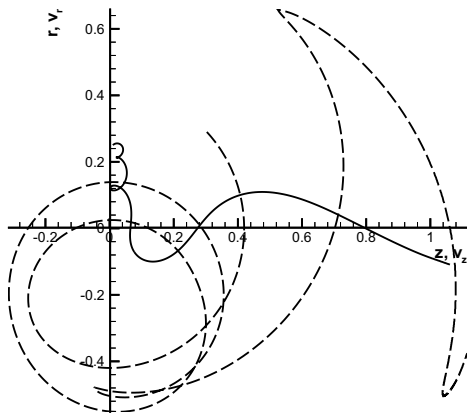
Fig. 8 Mixed orbit for ion close to the plasma border transiting to snake-like path having a high energy gain seen by velocity magnitude (dashed).
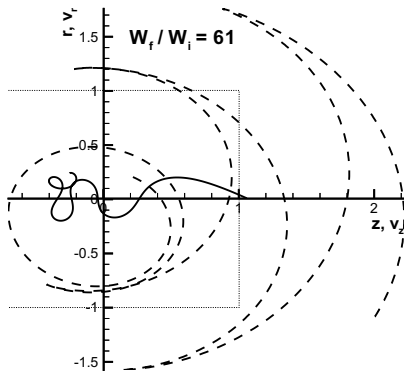

Fig. 9 Ion trajectory for a high-energy gain ion having mixed orbit, with initial energy 100 eV. Notice the large final velocity

gain is largest for mixed orbit ions, having increments larger than 60.

[1] M.G. Haines, Nuclear Instrum. Methods **207**, 179 (1983).
[2] M.J. Bernstein, Physics of Fluids **13**, 2858 (1970).
[3] R. Deutsch and W. Kies, Plasma Phys. Control. Fusion **30**, 263 (1988).
[4] B.A. Trubnikov, Fiz. Plazmy **12**, 468 (1986).
[5] V.V. Vikhrev, V.V. Ivanov and G.A. Rozanova, Fiz. Plazmy **15**, 77 (1989).
[6] Y.M. Shtemler and M. Mond, J. Plasma Phys. **72**, 699 (2006).